OPEN

PRS GLOBAL OPEN EXPERIMENTAL

Expression and Localization of Cathepsins B, D, and G in Dupuytren's Disease

Kirin Tan, MB ChB*
Helen D. Brasch, BMedSc, MBChB*
Bede van Schaijik, BTech (Hons)*
James R. Armstrong, MBBS, MD*†
Reginald W. Marsh, PhD*‡
Paul F. Davis, PhD*
Swee T. Tan, MBBS, PhD*†
Tinte Itinteang, MBBS, PhD*

Background: The pathogenesis of Dupuytren's disease (DD) remains unclear. An embryonic stem cell (ESC)–like population in the endothelium of the microvessels around tissues that expresses components of the renin-angiotensin system (RAS) has been reported. This study investigated if this primitive population expresses cathepsins B, D, and G, that contribute to RAS bypass loops.

Methods: 3,3-Diaminobenzidine immunohistochemical (IHC) staining for cathepsins B, D, and G was performed on sections of formalin-fixed paraffin-embedded DD cords (n = 10) and nodules (n = 10). Immunofluorescence IHC staining was utilized to demonstrate co-expression of these cathepsins with ESC markers. Protein and gene expression of these cathepsins was investigated in snap-frozen DD cords (n = 3) and nodules (n = 3) by Western blotting and NanoString analysis, respectively. Enzymatic activity of these cathepsins was investigated by enzymatic activity assays.

Results: 3,3-Diaminobenzidine IHC staining demonstrated expression of cathepsins B, D, and G in DD cords and nodules. Gene expression of cathepsins B, D, and G was confirmed by NanoString analysis. Western blotting confirmed expression of cathepsins B and D, but not cathepsin G. Immunofluorescent IHC staining demonstrated high abundance of cathepsins B and D on the OCT4$^+$/angiotensin converting enzyme$^+$ endothelium and the smooth muscle layer of the microvessels. Cathepsin G was localized to trypase$^+$ cells within the stroma in DD cords and nodules with limited expression on the microvessels. Enzyme activity assays demonstrated functional activity of cathepsins B and D.

Conclusions: Cathepsins B, D, and G were expressed in the DD tissues, with cathepsins B and D localized to the primitive population in the endothelium of the microvessels, whereas cathepsin G was localized to phenotypic mast cells, suggesting the presence of bypass loops for the RAS. *(Plast Reconstr Surg Glob Open 2018;6:e1686; doi: 10.1097/GOX.0000000000001686; Published online 14 February 2018.)*

INTRODUCTION

Dupuytren's disease (DD) is a fibro-proliferative disorder characterized by progressive palmar fascia fibrosis, with a variable prevalence that increases with age, predominantly affecting males of Northern European ancestry.[1,2] Although the risk factors for DD are well known, its pathogenesis remains unclear.

The development of thick collagenous cords that results in progressive fixed flexion contractures of the digits in DD leads to functional impairment. Management options for DD include steroid injections, collagenase injections and surgery.[3] The mainstay treatment of DD is surgery, most commonly fasciectomy, which is associated with recurrence, in up to 70% of patients.[4] The absence of an effective treatment for DD is underscored by the in-

*From the *Gillies McIndoe Research Institute, Wellington, New Zealand; †Wellington Regional Plastic, Maxillofacial & Burns Unit, Hutt Hospital, Wellington, New Zealand; and ‡University of Auckland, Auckland, New Zealand.*

Received for publication August 31, 2017; accepted January 5, 2018.

Presented at the New Zealand Association for Plastic Surgeons' and the Australian and New Zealand Society of Oculoplastic Surgeon's Joint Annual Scientific Meeting, Queenstown, New Zealand August 4–6, 2017.

Drs. Tan and Itinteang contributed equally to this work.

DOI: 10.1097/GOX.0000000000001686

Disclosure: Drs. Davis, Tan, and Itinteang are inventors of a patent application Treatment of Fibrotic Conditions (no. PCT/NZ2016/050187). The authors have no financial interest to declare in relation to the content of this article. The Article Processing Charge was paid for by the Gillies McIndoe Research Institute general fund.

Supplemental digital content is available for this article. Clickable URL citations appear in the text.

complete understanding of the pathogenesis of this common condition.[3,4]

Previous studies suggest mesenchymal stem cells (MSCs), which give rise to the proliferating myofibroblasts, are critical in the development of DD.[5,6] An embryonic stem cell (ESC)–like population within the endothelium of the microvessels surrounding the cords and nodules of DD has been identified.[7] This primitive population expresses components of the renin-angiotensin system (RAS), namely pro(renin) receptor, angiotensin converting enzyme (ACE), angiotensin II receptor 1 (ATIIR1) and angiotensin II receptor 2 (ATIIR2).[8] These findings suggest that dysfunction of the ESC-like population within the microvessels of DD may give rise to an intermediate MSC population, which in turn gives rise to the abundant downstream myofibroblasts—the dominant cell type within DD.[9] A putative role for the RAS in regulating this ESC-like population has been speculated, reminiscent of the findings in infantile hemangioma.[10]

The availability of ATII, the vasoactive downstream peptide of RAS pathway, may be promoted by cathepsins B, D, and G, proteases that contribute to RAS bypass loops.[11,12]

Cathepsin B, a cysteine protease produced as the inactive pro-cathepsin B, is homologous to renin.[11] It converts angiotensinogen (AGN) to ATI[13,14] and contributes to tumor invasion and metastasis.[15] Cathepsin B is also implicated in the development of glioblastoma,[16] rheumatoid arthritis,[17] and oral tongue squamous cell carcinoma.[18] Cathepsin D, an aspartyl protease, produced as the inactive pro-cathepsin D, is a homolog of renin.[14,15] It converts AGN to ATI[14,15] and is implicated in the formation of pulmonary[19] and renal[20] fibrosis. Cathepsin G, a serine proteinase, is converted from inactive pro-cathepsin G.[21,22] It is homologous to ACE, and it increases the availability of ATII from either AGN or ATI.[11,12] Stored in neutrophil granules, cathespin G is a proteolytic enzyme involved in immune defense and inflammation.[23]

In this study, we investigated the expression of cathepsins B, D, and G, and their localization in relation to the ESC-like population within DD[7] that expresses components of the RAS,[8] using immunohistochemical (IHC) staining, Western blotting (WB), and Nanostring mRNA analysis. We also investigated the function of these enzymes using enzyme activity assays.

METHODS

Tissue Samples

DD tissue samples from 10 male patients aged 66–78 (mean, 69.3) years including 6 patients used in our previous studies[7,8] were sourced from the Gillies McIndoe Research Institute Tissue Bank and used for this study that was approved by the Central Regional Health and Disability Ethics Committee (ref. no. 13NTB155). These DD samples were divided into cords and nodules by the operating surgeon (J.R.A.), which were processed for analysis separately. Written consent was obtained from all participants.

Histochemical and IHC Staining

Hematoxylin and eosin staining was performed on 4-μm-thick formalin-fixed paraffin-embedded sections of DD nodules and cords from 10 patients to confirm the presence of DD by an anatomical pathologist (H.D.B.). These sections underwent 3,3-diaminobenzidine (DAB) IHC staining. Antigen retrieval was performed using sodium citrate (Leica) at 95°C for 15 minutes. All sections underwent single DAB IHC staining with the primary antibodies, cathepsin B (1:1000; cat# sc-6490-R, Santa Cruz, Calif.), cathepsin D (1:200; cat# NCL-CDm, Leica, Wetzlar, Germany), cathepsin G (1:200; cat# sc-33206, Santa Cruz, Calif.), OCT4 (1:200; cat# NBPI-47923, Novus Biologicus, Littleton, Colo.), ACE (1:100; cat# 3C5, AbD Serotec, Oxford, United Kingdom), and tryptase (ready-to-use; cat# PA0019, Leica) with detection using the bond polymer refine detection kit (Leica).

Cords and nodules of 2 representative DD samples from the original cohort of 10 patients included in DAB IHC staining were selected for immunofluorescence (IF) IHC staining with the same primary antibodies at the same concentrations, but using a combination of Vectafluor Excel anti-mouse (ready-to-use; cat# VEDK2488, Vector Laboratories, Burlingame, Calif. or Alexa Fluor anti-rabbit 594 (1:500; cat# A21207, Life Technologies, Carlsbad, Calif.) as appropriate secondary antibodies. All antibodies were diluted in Bond primary antibody diluent (Leica), and all DAB and IF IHC staining were performed on the Leica Bond Rx auto-stainer (Leica, Nussloch, Germany). IF IHC stained slides were mounted using Vectashield hardset medium with DAPI (Vector Laboratories).

Positive controls included human placenta for cathepsin B,[24] epidermis of human skin for cathepsin D,[25] and mouse bone marrow for cathepsin G.[26] Negative controls for DAB IHC staining were performed on sections of DD cords and nodules using a matched isotype control for both mouse (ready-to-use; cat# IR750, Dako, Copenhagen, Denmark) and rabbit (ready-to-use; cat# IR600, Dako) primary antibodies, to determine the specificity of the amplification cascade. Negative controls for IF IHC staining were performed using a section of DD cord and nodule with the combined use of primary isotype mouse (ready-to-use; cat# IR750, Dako) and rabbit (ready-to-use; cat# IR600, Dako) antibodies.

Image Analysis

DAB IHC-stained slides were viewed and imaged using an Olympus BX53 microscope fitted with an Olympus DP21 digital camera (Olympus, Tokyo, Japan). IF IHC-stained slides were viewed and imaged using an Olympus FV1200 biological confocal laser-scanning microscope and processed with cellSens Dimension 1.11 software using 2D deconvolution algorithm (Olympus).

WB

Total protein was extracted from snap-frozen samples of DD cords and nodules from 3 of the original cohort of 10 patients used for DAB IHC staining, by pestle homogenization (cat# PES-15-B-SI, Corning, N.Y.) in ice-cold Radioimmunoprecipitation assay buffer buffer (cat#

R0278, Sigma-Aldrich, St. Louis, Mass.) supplemented with 1× HALT protease and phosphatase inhibitor cocktail (cat# 78440, Pierce Biotechnology, Rockford, Ill.) and 10 mM dithiothreitol (cat# 43816, Sigma-Aldrich). Soluble proteins were precipitated with ProteoExtract Protein Precipitation Kit (cat# 539180, Merck Millipore, Billerica, Mass.) and then resuspended at 70°C in Bolt 1× lithium dodecyl sulfate sample buffer (reduced sample) (cat# B0007, Thermo Fisher Scientific, Waltham, Mass.) at -20°C for 1 hour. Equal amounts of protein (~30 µg total protein per sample) were heated at 70°C and resolved by 4–12% 1D-PAGE (cat# NW04120BOX, Thermo Fisher Scientific) and transferred to a polyvinylidene fluoride membrane (cat# IB24001, Invitrogen, Carlsbad, Calif.) using an iBlot 2 (cat# IB21001, Thermo Fisher Scientific). Blotted membranes were blocked using 10 mL of 1× iBind Flex FD solution (cat# SLF2019, Thermo Fisher Scientific) for 5 minutes at room temperature and probed using the iBind Flex device (cat# SLF2000, Thermo Fisher Scientific) for cathepsin B (1:250; cat# SC-6490-R, Santa Cruz), cathepsin D (1:250; cat# SC-6486, Santa Cruz), cathepsin G (1:250; cat# ab197354, Abcam, Cambridge, United Kingdom), and β-actin (1:500; cat# ab8226 and ab8229, Abcam). Appropriate secondary antibodies were goat anti-rabbit Alexa Fluor 647 (1:2000; cat# A21244, Life Technologies) for cathepsins B and D, chicken anti-goat Alexa Fluor 647 (1:2000; cat# A21469, Life Technologies) for β-actin ab8229, goat anti-mouse Alexa Fluor 488 (1:2000; cat# A21202, Life Technologies) for β-actin ab8226, and goat anti-rabbit horseradish peroxidase (1:2000; cat# ab6721, Abcam) for cathepsin G. Clarity Western ECL (cat# 1705061, Bio-Rad) was used as the substrate for visualizing horseradish peroxidase detected protein bands and the Chemi Doc MP Imaging System (Bio-Rad) and Image Lab 5.0 software (Bio-Rad) were used for band detection and analysis. All experiments were performed in triplicate. Snap-frozen tonsillar tissue was used as control tissue for cathepsin B[27] and cathepsin D[28] and a recombinant cathepsin G protein (cat# H00001511-Q01, Novus Biologicals, Littleton, Colo.) was used as an appropriate positive control. Matched mouse (1:500; cat# ab18443, Abcam) and rabbit (1:500; cat# ab171870, Abcam) isotype controls were used as appropriate negative controls.

Enzymatic Activity Assay

Enzymatic activities of cathepsin B and cathepsin D were determined in snap-frozen DD cords and nodules from the same 3 patients used in the WB, using enzymatic activity assay kits for cathepsin B (cat# ab65300; Abcam) and cathepsin D (cat# ab65302; Abcam). All steps of the procedure were performed according to the manufacturer's protocol. Fluorescence was measured in a Nunc F96 MicroWell black polystyrene plate (cat# 136101, Thermo Fisher Scientific) using the Varioskan Flash plate reader (cat# MIB5250030, Thermo Fisher Scientific). Tonsil and denatured tonsil tissue lysates were used as appropriate positive and negative controls, respectively.

Nanostring MRNA Analysis

Snap-frozen samples of DD cords and nodules from the same 3 patients subjected to WB and enzymatic activity assays were used to isolate total RNA for NanoString nCounter Gene Expression Assay (NanoString Technologies, Seattle, Wash.). RNA was extracted from frozen tissues using RNeasy Mini Kit (Qiagen) and subjected to the NanoString nCounter gene expression assay by New Zealand Genomics Ltd (Dunedin, New Zealand). The probes for the genes encoding cathepsin B (CTSB; NM_001908.3), cathepsin D (CTSD; NM_001909.3), cathepsin G (CTSG; NM_001911.2), and the housekeeping gene GUSB (NM_00181.3) were used. Raw data were analyzed by nSolver software (NanoString Technologies) using standard settings and were normalized against the housekeeping gene.

Statistical Methods

GraphPad (QuickCalcs) software for *t* test was used to analyze the NanoString data.

Ethics Approval

Central Regional Health and Disability Ethics Committee (ref. no. 13NTB155).

RESULTS

Histochemical and DAB IHC Staining

DAB IHC staining demonstrated expression of cathepsin B (Supplemental Digital Content 1 A and B, brown), cathepsin D (**Supplemental Digital Content 1** C and D, brown) and cathepsin G (**Supplemental Digital Content 1** E and F, brown) in DD cords (**Supplemental Digital Content 1** A, C, and E) and nodules (**Supplemental Digital Content 1** B, D, and F). Cathepsin B and cathepsin D were localized to the endothelium and the smooth muscle layer of the microvessels [**see figure,** Supplemental Digital Content 1, which displays representative DAB IHC-stained sections of DD cords (A, C, and E) and DD nodules (B, D, and F), ***http://links.lww.com/PRSGO/A682***]. Expression of cathepsin G was primarily localized to a small number of cells within the stroma with limited expression on the endothelium and smooth muscle of the microvessels. There was no observable difference in the expression of each cathepsin in the DD cords and nodules.

Positive controls for cathepsins B, D, and G demonstrated appropriate staining in human placenta (**Supplemental Digital Content 2**A, brown), epidermis of human skin (**Supplemental Digital Content 2**, brown), and mouse bone marrow (**Supplemental Digital Content 2**C, brown), respectively. The negative control demonstrated minimal staining [**Supplemental Digital Content 2**D, brown; **see figure,** Supplemental Digital Content 2, which displays positive controls of DAB IHC staining for cathepsin B (A, brown), cathepsin D (B, brown), and cathepsin G (C, brown) demonstrated on sections of human placenta, epidermis of human skin and mouse bone marrow, respectively, ***http://links.lww.com/PRSGO/A683***].

IF IHC Staining

IF IHC staining was performed to determine the localization of each cathepsin in relation to the ESC-like population within DD tissue[7] that expresses the components of the RAS.[8] Cathepsin B (Fig. 1A, D, red) and cathepsin D

(Fig. 1B, E, red) but not cathepsin G (Fig. 1C, F, red) were expressed by the OCT4$^+$ ESC-like population (Fig. 1A–F, green) on the endothelium of the microvessels in DD cords (Fig. 1A–C) and DD nodules (Fig. 1D–F). Cathepsin G (Fig. 1C, red) was localized to the OCT4$^+$ (Fig. 1C, green) cells located within the stroma, away from the microvessels in both the DD cords (Fig. 1C) and DD nodules (Fig. 1F). Cathepsin B (Fig. 2A, D, red) and cathepsin D (Fig. 2B, E, red), but not cathepsin G (Fig. 2C, F, red) were expressed by the ACE$^+$ (Fig. 2A–F, green) endothelium, in both DD cords (Fig. 2A–C) and DD nodules (Fig. 2D–F). Cathepsin G (Fig. 2G, H, red) was localized to cells within the stroma that expressed tryptase (Fig. 2G, H, green) in both DD cords (Fig. 2G) and DD nodules (Fig. 2H), similar to the phenotypic mast cells in infantile hemangioma.[10]

Split images in Figure 1 and Figure 2 are shown in **Supplemental Digital Content 3** and **Supplemental Digital Content 4**, respectively (**see figure,** Supplemental Digital Content 3, which displays split images of IF IHC-stained images shown in Fig. 2A–F, ***http://links.lww.com/PRSGO/A680***; **see figure,** Supplemental Digital Content 4, which displays split images of IF IHC-stained images shown in Fig. 3A–H, ***http://links.lww.com/PRSGO/A681***). The negative controls for IF IHC staining demonstrated minimal staining in a DD cord (**Supplemental Digital Content 4**Q) and a DD nodule (**Supplemental Digital Content 4**R), as expected.

Nanostring MRNA Analysis

NanoString mRNA analysis for cathepsins B, D, and G, normalized against the housekeeping gene GUSB, confirmed transcriptional activation for all the aforementioned genes in both DD cords and nodules (Fig. 3). The average expression of cathepsin B, in both DD cords and nodules, was significantly greater than that of cathepsin D ($P = 0.02$), and the average expression of cathepsin D was significantly greater than that of cathepsin G ($P = 0.004$).

WB

WB of the snap-frozen samples of DD cord (n = 3) and nodule (n = 3) demonstrated the presence of bands at the expected molecular weight for cathepsin B (Fig. 4A) and cathepsin D (Fig. 4B). Cathepsin B was detected at the appropriate molecular weight of 25 kDa[31] in all 3 DD nodule samples and 2 out of 3 DD cord samples. Cathepsin D was detected at 28 kDa[35] in all 3 DD nodule samples and 3 DD cord samples. Cathepsin G was not detected in any of the DD tissue samples at the expected molecular weight of 29 kDa[36] (Fig. 4C), with specificity of the antibody confirmed in the positive control, which demonstrated detection of a band at the expected molecular weight of 37 kDa,

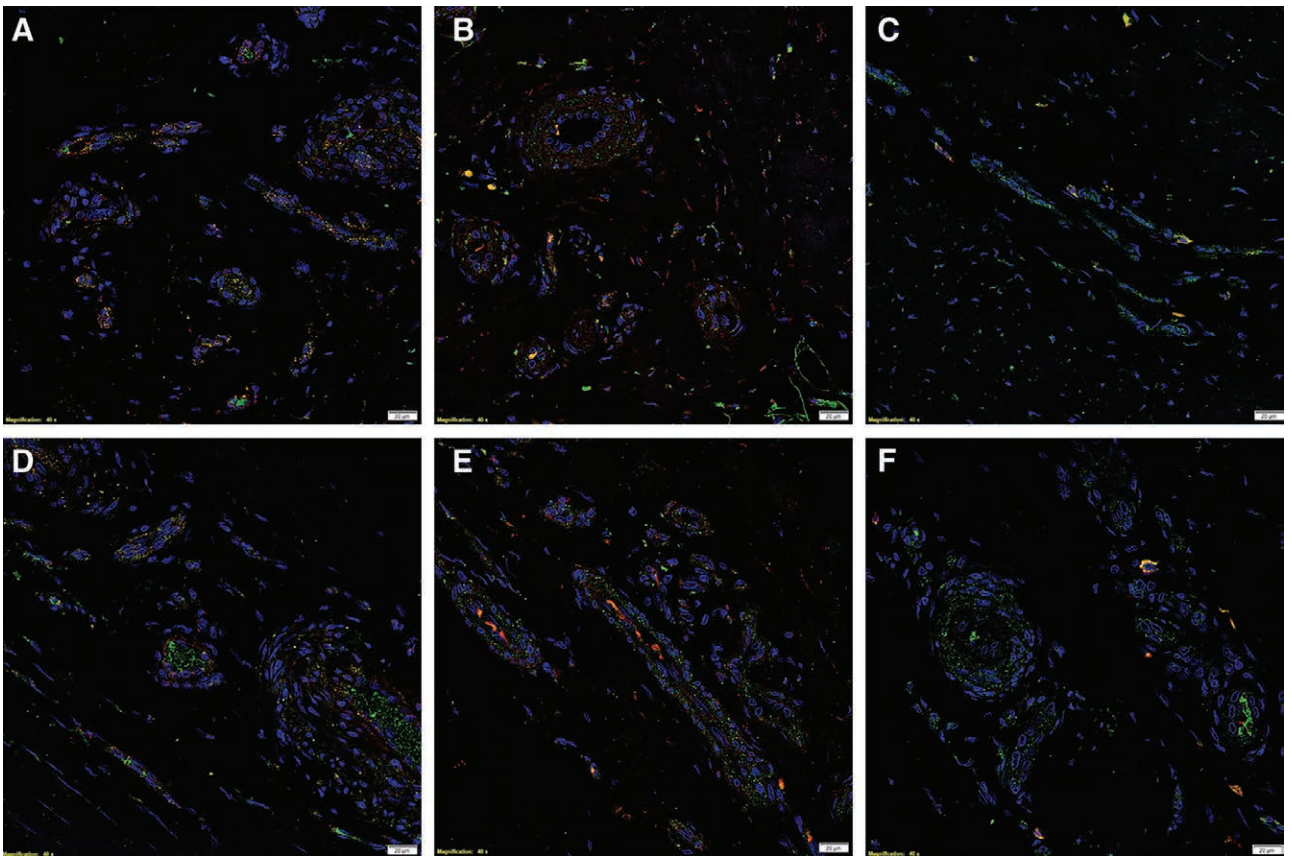

Fig. 1. Representative IF IHC-stained sections of DD cords (A–C) and DD nodules (D–F) demonstrating expression of cathepsin B (A and D, red), cathepsin D (B and E, red) but not cathepsin G (C and F, red) on the OCT4$^+$ (A–F, green) endothelium of the microvessels. Cathepsin G (C and F, red) was expressed by cells within the stroma, away from the OCT4$^+$ (C and F, green) microvessels. Cell nuclei (A–F, blue) were counter-stained with 4′, 6′-diamino-2-phenylindole. Scale bars: 20 μm.

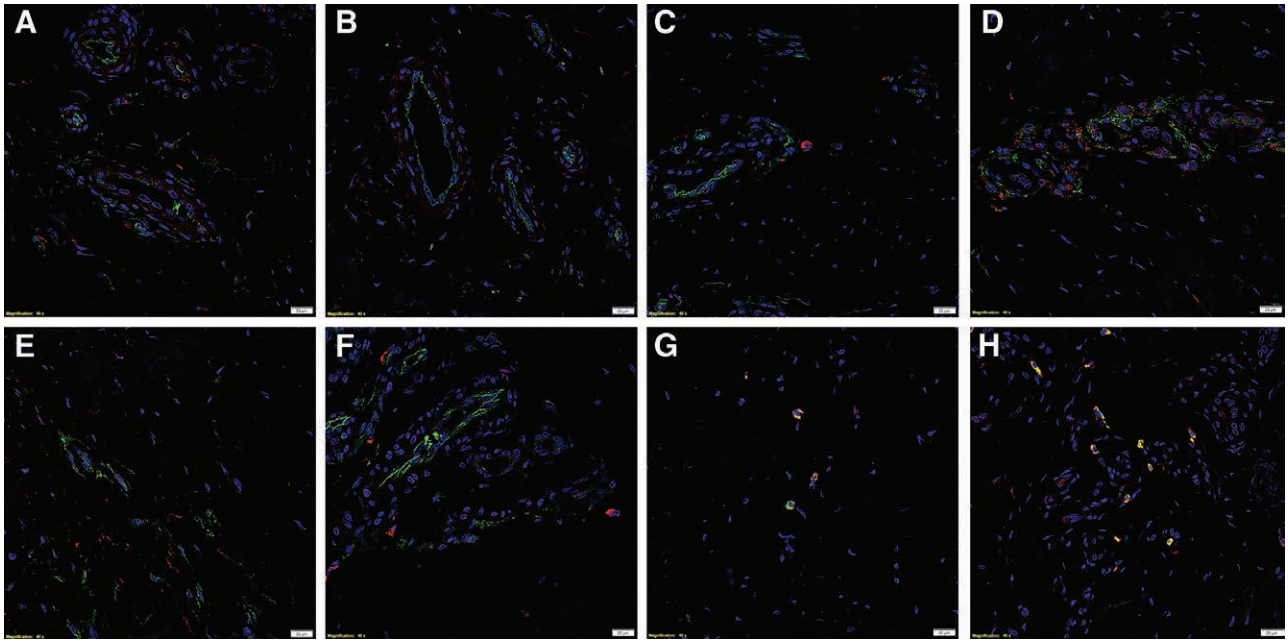

Fig. 2. Representative IF IHC-stained sections of DD cords (A–C, G) and DD nodules (D–F, H) demonstrating the expression of cathepsin B (A and D, red), cathepsin D (B and E, red) but not cathepsin G (C and F) on the ACE^{+} (A–F, green) endothelium of the microvessels. Cathepsin G (G and H, red) was expressed by cells within the stroma that expressed tryptase (G and H, green). Cell nuclei (A–H) were counter-stained with 4′, 6′-diamino-2-phenylindole. Scale bars: 20 µm.

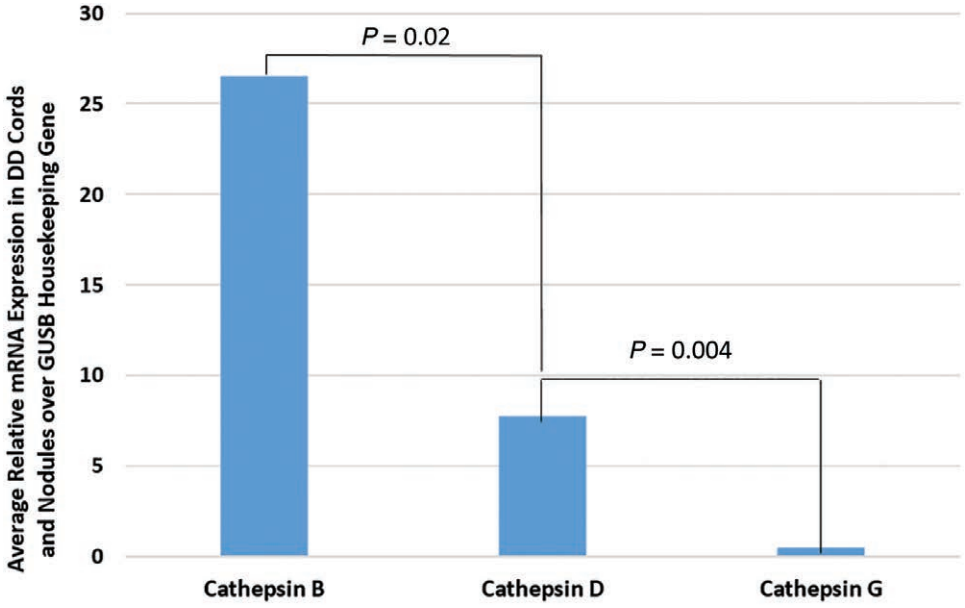

Fig. 3. Average relative expression of mRNA transcripts of cathepsins B, D, and G in DD in 6 patients. Expression is depicted in relative units as a ratio to the GUSB housekeeper gene.

consistent with the supplier's product information. β-actin (Fig. 4A–C) confirmed equivalent protein loading for all 3 DD cord and nodule samples examined.

Enzymatic Activity Assays

To determine the functional activity of both cathepsin B and cathepsin D, which were detected by WB, we performed enzymatic activity analysis on the same snap-frozen DD tissue samples, for both cathepsins. All DD cord and nodule samples demonstrated enzymatic activity of cathepsin B and cathepsin D relative to that of the positive and negative control tissues (Fig. 5).

DISCUSSION

Previous studies suggest MSCs may give rise to the proliferating myofibroblasts, a hallmark of fibrosis, characteristic of DD.[5,6] A putative upstream ESC-like population within

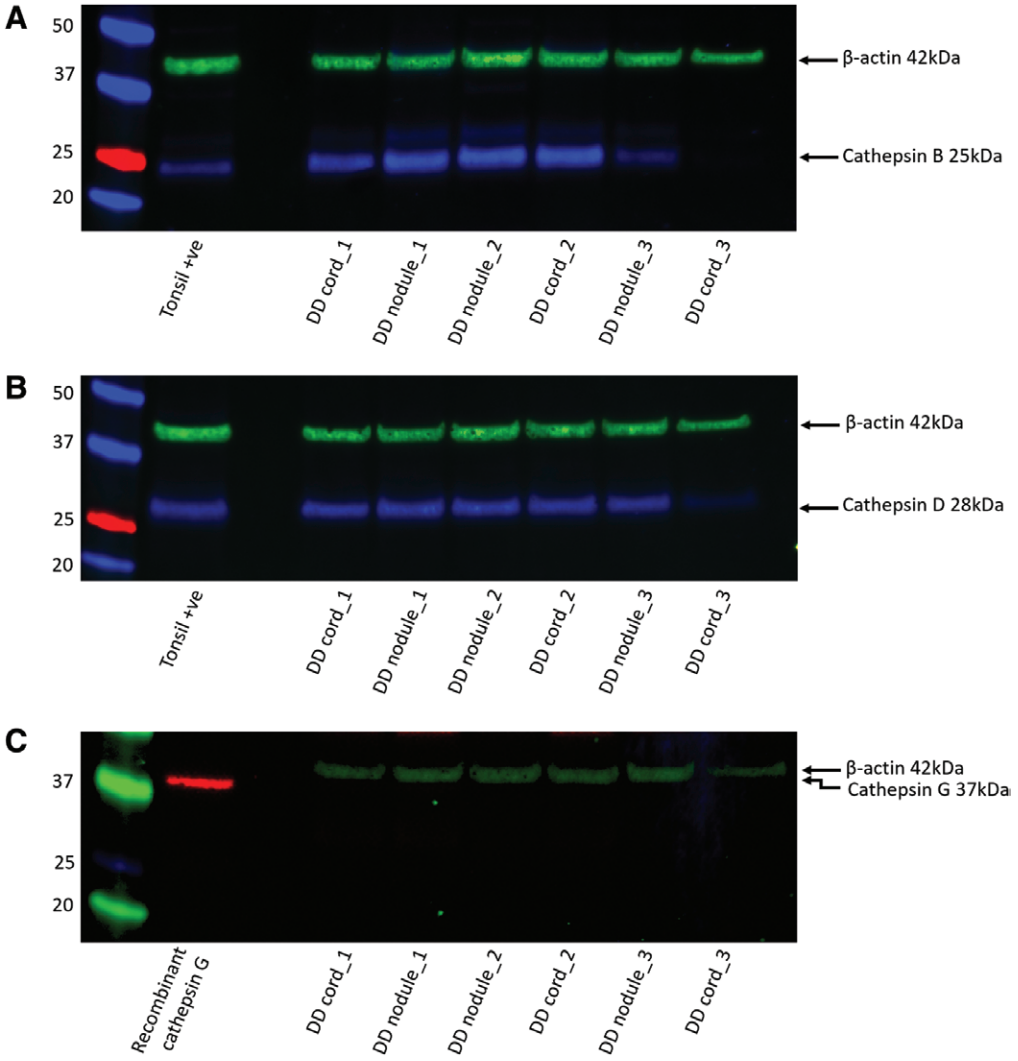

Fig. 4. Representative WB images of total protein extracted from 3 DD cords and 3 DD nodules from 3 patients demonstrating the presence of cathepsin B (A), cathepsin D (B), but not cathepsin G (C). β-actin confirmed approximately equivalent protein load between samples.

DD tissue[7] has been demonstrated, and it has been suggested that this primitive population may give rise to the MSCs previously identified.[5] This ESC-like population expresses components of the RAS: pro(renin) receptor, ACE, ATIIR1, and ATIIR2, suggesting a crucial role for the RAS in the pathogenesis of DD.[8] To the best of our knowledge, this is the first study that demonstrates the expression of cathepsins B, D, and G in both DD cords and nodules.

Cathepsins B, D, and G are proteases that contribute to bypass loops of the RAS (Fig. 6). Cathepsin B that converts pro-renin to renin, is synthesized as pro-cathepsin B, an inactive pro-enzyme, with a molecular weight of 37–39 kDa.[29,30] Pro-cathepsin B is activated by endogenous aspartic proteinases, or through autocatalysis in acidic conditions (pH, 4.5–5.5)[30,32] and is subsequently converted to cathepsin B, which consists of a 30 kDa single chain and a 25–26 kDa heavy chain doublet.[33,34]

Similarly, cathepsin D converts AGN to ATI, and it is initially produced as pro-cathepsin D with a molecular weight of 52 kDa. Pro-cathepsin D is then converted in the endoplasmic reticulum by renin or pH-dependent autocatalysis, resulting in the mature form of cathepsin D, consisting of a 28 kDa heavy chain and a 14 kDa light chain.[35]

Cathepsin G converts AGN to ATI or ATII and is produced from a precursor pro-cathepsin G, with a molecular weight of 32.5 kDa. Pro-cathepsin G is converted to active cathepsin G of 29–30 kDa, by the proteolytic activity of cathepsin C.[36]

The expression of cathepsins B, D, and G demonstrated by IHC staining was confirmed by NanoString mRNA analysis. We have also shown significantly higher transcript expression of cathepsin B than cathepsin D, with both being significantly more abundant than that of cathepsin G.

The protein expression of cathepsin B and cathepsin D was also confirmed by WB and enzymatic activity assays demonstrated functional activity of these cathepsins. IHC staining demonstrated expression and localization of cathepsin G to very few cells within DD cords and nodules. It is therefore not surprising that cathepsin G was below detectable levels by WB.

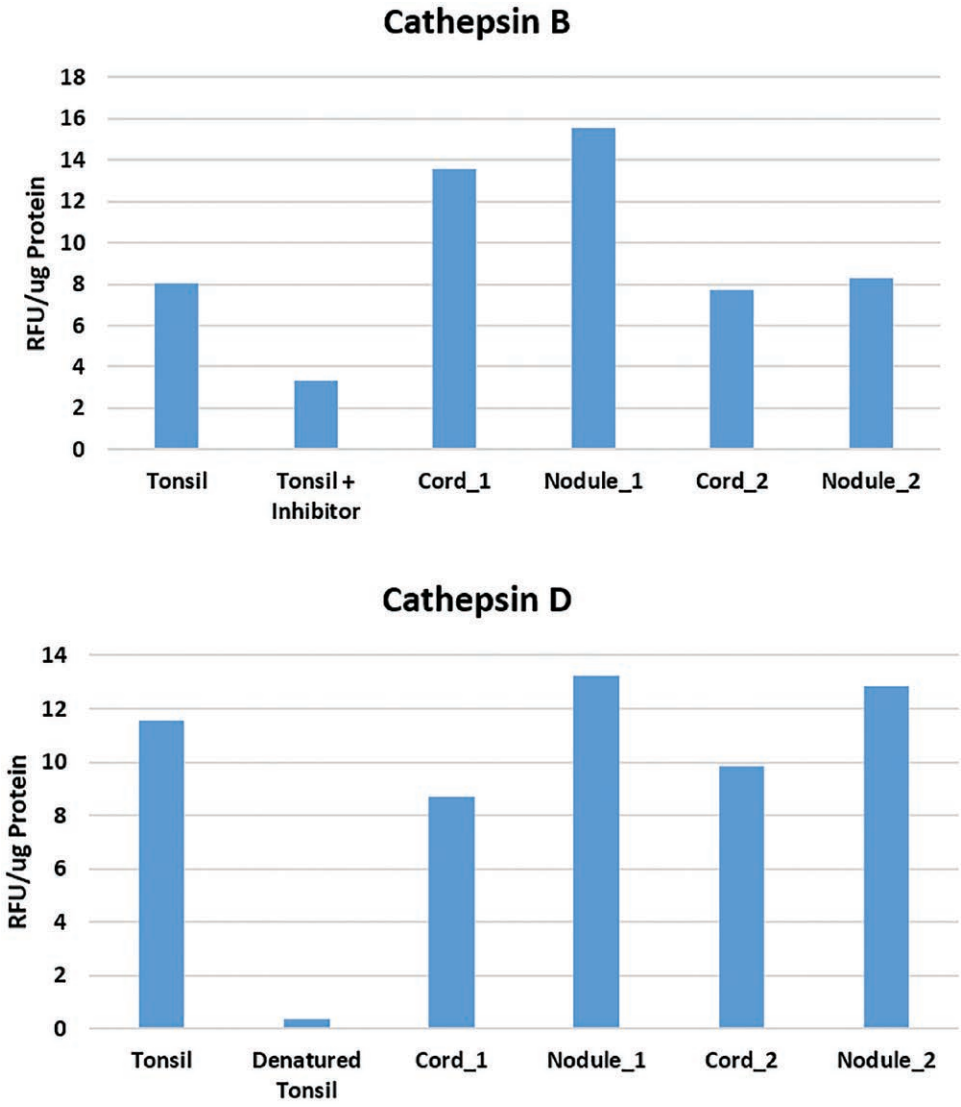

Fig. 5. Enzymatic activity assays on DD cord and DD nodule samples showing activity of cathepsin B and cathepsin D per µg of protein in lysate, relative to positive and negative controls. The activity is expressed as relative fluorescent unit (RFU).

IF IHC staining demonstrated that cathepsin B and cathepsin D were expressed by the ESC-like population within the endothelium of the microvessels that expresses the ESC marker OCT4, and ACE, a component of the RAS. We infer that these cathepsins may provide bypass loops for the RAS, thus increasing the availability of ATII.

Mast cells have been shown to be overexpressed in DD tissue suggesting a role in this condition.[37] The demonstration of expression of cathepsin G by the $OCT4^{+}$ mast cells within the DD cords and nodules is novel, similar to the observation in proliferating infantile hemangioma.[10] Cathepsin G, along with other proteases, is released from mast cells following stimulation by agents such as substance P.[37] Apart from contributions to a bypass loop in the RAS, cathepsin G possesses other actions[38] although its precise role in DD remains unclear.

The expression of components of the RAS by the ESC-like population in the microvessels within DD tissue[8] suggests a crucial role of the RAS in the regulation of the primitive population, which may then differentiate into the mesenchymal progenitors, through an endothelial-to-mesenchymal transition.[39,40] This ESC-like population may be a novel therapeutic target through modulation of the RAS using existing medications. This hypothesis is supported by the observation of improvement in fibrotic conditions, such as keloid scar, following administration of low-dose enalapril, an ACE inhibitor.[41,42]

In conclusion, we have demonstrated that cathepsin B and cathepsin D are abundantly expressed by the ESC-like population in the endothelium of the microvessels surrounding DD cords and nodules, and that these cathepsins are functionally active. We have also shown that cathepsin G is expressed by the phenotypically primitive mast cells within DD although its expression is minimal. We infer that cathepsin B and cathepsin D, and potentially cathepsin G, may provide bypass loops for the RAS expressed by the ESC-like population.

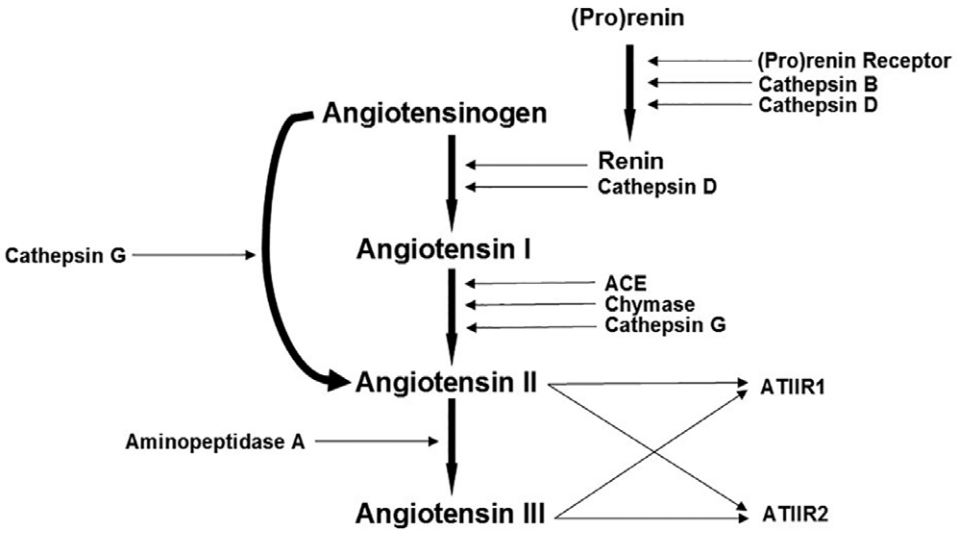

Fig. 6. Schema demonstrating the RAS and the role of cathepsins B, D, and G. AGN is converted to ATI by renin, which is subsequently converted to ATII by ACE. ATII is converted to ATIII by the actions of aminopeptidase A. ATII and ATIII then act on ATIIR1 and ATIIR2. Cathepsins B and D catalyze the conversion of renin from (pro)renin; cathepsin D leads to the production of ATI from AGN; chymase enhances the production of ATII from ATI, whereas cathepsin G leads to ATII production from either AGN or ATI. Reproduced with permission from *Frontiers of Surgery.*[16]

Although beyond the scope of this report, it is exciting to speculate on the possibility of targeting the ESC-like population within DD using RAS modulators, such as ACE inhibitors as previously proposed[43] and inhibitors of cathepsins, such as curcumin[44] for cathepsin B, pepstatin for cathepsin D,[45] and chymostatin[45] for cathepsin G, in the treatment of this condition.

Swee T. Tan, ONZM, MBBS, PhD, FRACS
Gillies McIndoe Research Institute
PO Box 7184, Newtown 6242
Wellington, New Zealand
E-mail: swee.tan@gmri.org.nz

ACKNOWLEDGMENTS

The authors thank Ms. Liz Jones and Ms. Alice Chibnall of the Gillies McIndoe Research Institute for their assistance in IHC staining and performing tissue processing for NanoString analysis, respectively.

REFERENCES

1. Hindocha S, McGrouther DA, Bayat A. Epidemiological evaluation of Dupuytren's disease incidence and prevalence rates in relation to etiology. *Hand (N Y).* 2009;4:256–269.
2. Geoghegan JM, Forbes J, Clark DI, et al. Dupuytren's disease risk factors. *J Hand Surg Br.* 2004;29:423–426.
3. Riester S, van Wijnen A, Rizzo M, et al. Pathogenesis and treatment of Dupuytren disease. *JBJS Rev.* 2014;2:e2. doi:10.2106/JBJS.RVW.M.00072.
4. Becker GW, Davis TR. The outcome of surgical treatments for primary Dupuytren's disease—a systematic review. *J Hand Surg Eur Vol.* 2010;35:623–626.
5. Hindocha S, Iqbal SA, Farhatullah S, et al. Characterization of stem cells in Dupuytren's disease. *Br J Surg.* 2011;98:308–315.
6. Iqbal SA, Manning C, Syed F, et al. Identification of mesenchymal stem cells in perinodular fat and skin in Dupuytren's disease: a potential source of myofibroblasts with implications for pathogenesis and therapy. *Stem Cells Dev.* 2012;21:609–622.
7. Koh SP, On N, Brasch HD, et al. Embryonic stem cell-like population in Dupuytren's disease. *Plast Reconstr Surg Glob Open.* 2016;4:e1064.
8. On N, Koh SP, Brasch HD, et al. Embryonic stem cell-like population in Dupuytren's disease expresses components of the renin-angiotensin system. *Plast Reconstr Surg Glob Open.* 2017;5:e1422.
9. Shih B, Bayat A. Scientific understanding and clinical management of Dupuytren disease. *Nat Rev Rheumatol.* 2010;6:715–726.
10. Itinteang T, Chudakova DA, Dunne JC, et al. Expression of cathepsins B, D, and G in infantile hemangioma. *Front Surg.* 2015;2:26.
11. Neves FA, Duncan KG, Baxter JD. Cathepsin B is a prorenin processing enzyme. *Hypertension.* 1996;27:514–517.
12. Munro MJ, Wickremesekera AC, Davis PF, et al. Renin-angiotensin system and cancer: a review. *Integr Cancer Sci Ther.* 2017;4:1–6. doi:10.15761/ICST.1000231.
13. Naseem RH, Hedegard W, Henry TD, et al. Plasma cathepsin D isoforms and their active metabolites increase after myocardial infarction and contribute to plasma renin activity. *Basic Res Cardiol.* 2005;100:139–146.
14. Graciano ML, Cavaglieri Rde C, Dellê H, et al. Intrarenal renin-angiotensin system is upregulated in experimental model of progressive renal disease induced by chronic inhibition of nitric oxide synthesis. *J Am Soc Nephrol.* 2004;15:1805–1815.
15. MacKenzie JR, Mason SL, Hickford JG, et al. A polymorphic marker for the human cathepsin B gene. *Mol Cell Probes.* 2001;15:235–237.
16. Koh SP, Wickremesekera AC, Brasch HD, et al. Expression of cathepsins B, D, and G in isocitrate dehydrogenase-wildtype glioblastoma. *Front Surg.* 2017;4:28.
17. Hashimoto Y, Kakegawa H, Narita Y, et al. Significance of cathepsin B accumulation in synovial fluid of rheumatoid arthritis. *Biochem Biophys Res Commun.* 2001;283:334–339.
18. Featherston T, Marsh RW, van Schaijik B, et al. Expression and localization of cathepsins B, D, and G in two cancer stem cell sub-

populations in moderately differentiated oral tongue squamous cell carcinoma. *Front Med (Lausanne).* 2017;4:100.
19. Kasper M, Lackie P, Haase M, et al. Immunolocalization of cathepsin D in pneumocytes of normal human lung and in pulmonary fibrosis. *Virchows Arch.* 1996;428:207–215.
20. Fox C, Cocchiaro P, Oakley F, et al. Inhibition of lysosomal protease cathepsin D reduces renal fibrosis in murine chronic kidney disease. *Sci Rep.* 2016;6:20101.
21. Salvesen G, Farley D, Shuman J, et al. Molecular cloning of human cathepsin G: structural similarity to mast cell and cytotoxic T lymphocyte proteinases. *Biochemistry.* 1987;26:2289–2293.
22. Gullberg U, Lindmark A, Nilsson E, et al. Processing of human cathepsin G after transfection to the rat basophilic/mast cell tumor line RBL. *J Biol Chem.* 1994;269:25219–25225.
23. Pham CT. Neutrophil serine proteases: specific regulators of inflammation. *Nat Rev Immunol.* 2006;6:541–550.
24. Crocker J, Burnett D, Jones EL. Immunohistochemical demonstration of cathepsin B in the macrophages of benign and malignant lymphoid tissues. *J Pathol.* 1984;142:87–94.
25. Horikoshi T, Arany I, Rajaraman S, et al. Isoforms of cathepsin D and human epidermal differentiation. *Biochimie.* 1998;80:605–612.
26. Grisolano JL, Sclar GM, Ley TJ. Early myeloid cell-specific expression of the human cathepsin G gene in transgenic mice. *Proc Natl Acad Sci U S A.* 1994;91:8989–8993.
27. Howie AJ, Burnett D, Crocker J. The distribution of cathepsin B in human tissues. *J Pathol.* 1985;145:307–314.
28. Whitaker JN, Rhodes RH. The distribution of cathepsin D in rat tissues determined by immunocytochemistry. *Am J Anat.* 1983;166:417–428.
29. Santa Cruz Biotechnology. Cathepsin B (S-12): sc-6493. Available at http://datasheets.scbt.com/sc-6493.pdf. Accessed June 18, 2017.
30. Kawabata T, Nishimura Y, Higaki M, et al. Purification and processing of rat liver procathepsin B. *J Biochem.* 1993;113:389–394.
31. Mach L, Mort JS, Glössl J. Maturation of human procathepsin B. Proenzyme activation and proteolytic processing of the precursor to the mature proteinase, *in vitro*, are primarily unimolecular processes. *J Biol Chem.* 1994;269:13030–13035.
32. Olson OC, Joyce JA. Cysteine cathepsin proteases: regulators of cancer progression and therapeutic response. *Nat Rev Cancer.* 2015;15:712–729.
33. Moin K, Day NA, Sameni M, et al. Human tumour cathepsin B. Comparison with normal liver cathepsin B. *Biochem J.* 1992;285:427–434.
34. Ritonja A, Popovic T, Turk V, et al. Amino acid sequence of human liver cathepsin B. *FEBS Lett.* 1985;181:169–172.
35. Rijnboutt S, Kal AJ, Geuze HJ, et al. Mannose 6-phosphate-independent targeting of cathepsin D to lysosomes in HepG2 cells. *J Biol Chem.* 1991;266:23586–23592.
36. Korkmaz B, Moreau T, Gauthier F. Neutrophil elastase, proteinase 3 and cathepsin G: physicochemical properties, activity and physiopathological functions. *Biochimie.* 2008;90:227–242.
37. Schubert TE, Weidler C, Borisch N, et al. Dupuytren's contracture is associated with sprouting of substance P positive nerve fibres and infiltration by mast cells. *Ann Rheum Dis.* 2006;65:414–415.
38. Caughey GH. Mast cell tryptases and chymases in inflammation and host defense. *Immunol Rev.* 2007;217:141–154.
39. Mani SA, Guo W, Liao MJ, et al. The epithelial-mesenchymal transition generates cells with properties of stem cells. *Cell.* 2008;133:704–715.
40. Polyak K, Weinberg RA. Transitions between epithelial and mesenchymal states: acquisition of malignant and stem cell traits. *Nat Rev Cancer.* 2009;9:265–273.
41. Iannello S, Milazzo P, Bordonaro F, et al. Low-dose enalapril in the treatment of surgical cutaneous hypertrophic scar and keloid-two case reports and literature review. *Med Gen Med.* 2006;8:60. Available at http://www.medscape.com/viewarticle/548554._1. Accessed June 8, 2017.
42. Knobloch K, Redeker J, Vogt PM. Antifibrotic medication using a combination of N-acetyl-L-cystein (NAC) and ACE inhibitors can prevent the recurrence of Dupuytren's disease. *Med Hypotheses.* 2009;73:659–661.
43. Stephen C, Touil L, Vaiude P, et al. Angiotensin receptors in Dupuytren's disease: a target for pharmacological treatment? *J Plast Surg Hand Surg.* 2017:1–3. doi:10.1080/2000656X.2017.1319846.
44. Ravish I, Raghav N. Curcumin as inhibitor of mammalian cathepsin B, cathepsin H, acid phosphatase and alkaline phosphatase: a correlation with pharmacological activities. *Med Chem Res.* 2014;23:2847–2855. doi:10.1007/s00044-013-0872-1.
45. Agarwal SK. Proteases cathepsins—a view. *Biochem Educ.* 1990;18:67–72. doi:10.1016/0307-4412(90)90176-O.